IOP Conference Series: Earth and Environmental Science

Modeling and Comparison of Data Obtained by GPR, for Geological / Structural Analysis of a Carbonated Ornamental Rock Quarry - Blocometry Validation - Case Study in Valinho De Fátima, Portugal

To cite this article: João Duarte *et al* 2020 *IOP Conf. Ser.: Earth Environ. Sci.* **609** 012068

Modeling and Comparison of Data Obtained by GPR, for Geological / Structural Analysis of a Carbonated Ornamental Rock Quarry - Blocometry Validation - Case Study in Valinho De Fátima, Portugal

João Duarte[1], Marco Cunha[2], José Carvalho[3]

[1]IQGeo-Serviços, Lda., Coimbra, Portugal, University of Coimbra, Geosciences Center, Coimbra, Portugal

[2]GeoSurveys, Lda., Luanda, Angola

[3]University of Coimbra, Department of Earth Sciences, Coimbra, Portugal

joao.aduarte@iqgeo.pt

Abstract. Portugal, in the continental and insular territory, has raw geological resources in diversity and quality that are materials for the manufacturing industries, particularly linked to the civil construction, architecture and public works with great weight in its exports, revealing to be one big producer of ornamental stones worldwide. In this industry, the presence of discontinuities, grain size, colour, textural anisotropy and porosity are factors that can determine the economic viability of the exploitations. For this, it is important to develop effective prospecting routines that allow the geological/structural fast analysis and economic potential assessment of the massifs and subsequent correct planning and dimensioning of the exploitations. This work intends to model and integrate data from the ground penetration radar (GPR), together with close-range photogrammetry, derived from an Unmanned aerial vehicle (UAV) imagery. The objective is to identify and determine the spatial distribution of the various elements by modelling the acquired data, as well as verifying the feasibility of the technical disassembly option adopted. We have used GPR as it is non-destructive, fast to deploy, survey, process and interpret. The acquired data were processed using the GPR-SLICE, where a 3D final dataset was obtained and interpreted. GPR and photogrammetric model was integrated and interpreted and validated with direct field observations. The model obtained showed in its upper part, an area corresponding to the presence of sludge from the cut of the rock, followed by a strip that corresponds to the oolitic limestone. Further down to the end of the block, the presence of oolitic limestone with crossed stratification is identifiable. There was a textural and structural correspondence between the GPR data and direct field observations. GPR did not reveal any major morphostructural discontinuity, validating the technical option of choosing the places where the cuts were made for their individualization, as the block was cut clean. The GPR and photogrammetry data integration method revealed to be complementary, where results were obtained easily, fast, and with centimeter accuracy. The same methodology presented, revealed to be cheap and effective for both localized studies and optimization of the overall quarry's extraction plan and design.

1. Introduction

State in the ornamental rock industry, it is important to characterize and locate, in the exploration phase, the areas where the massif will be dismantled, considering the characteristics that give them most commercial value [1].

For this to be economically viable, it is necessary to meet some requirements related to the presence of discontinuities, size or presence of grains, structural anisotropy, and porosity of materials [2] [3], as well as their location and extent in the massif.

The presence or not of these elements in the rocky massif is an economic risk factor, which must be identified previously [4], determining the technical and economic viability of the exploration. This preliminary work intends, with the use of non-destructive geophysical methods, reveal a methodology that allows to reduce costs and rigorously, detect, quantify and model these hidden subsurface characteristics (discontinuity [3, 5, 6], the variety of types and textures of rocks, horizontal and vertical development [7]) and position them in the massif, since pre-detection presents some degree of difficulty and generally uses intrusive and expensive techniques.

The aim of this study is to validate, in the exploration phase, the use of a methodology that uses non-destructive techniques, in the evaluation of the rocky massif. The use of the ground-penetrating radar (GPR) method, integrated with aerophotogrammetric surveys and 3D modelling. This is objectively a competitive advantage, which allows professionals involved in the sector to identify and quantify the risk factors that allow the implementation of the exploitation or minimization of associated risks. It increases the possibility of exploiting quality products, avoiding as much as possible their waste, reducing the costs associated with exploration, through the proper planning of the exploiting.

2. Spatial and geologic framework

The present work was carried out in a quarry located in the center of Portugal, at Valinho de Fátima, Fátima, whose location is indicated in figure 1 [8-9]. Geologically the outcrop limestones are stratigraphically located in the middle Jurassic – Callovian, Formation of Santo António - Candeeiros - Member of Moleanos) [10], formed by oolitic, biocalciclastic and sparritic limestones.

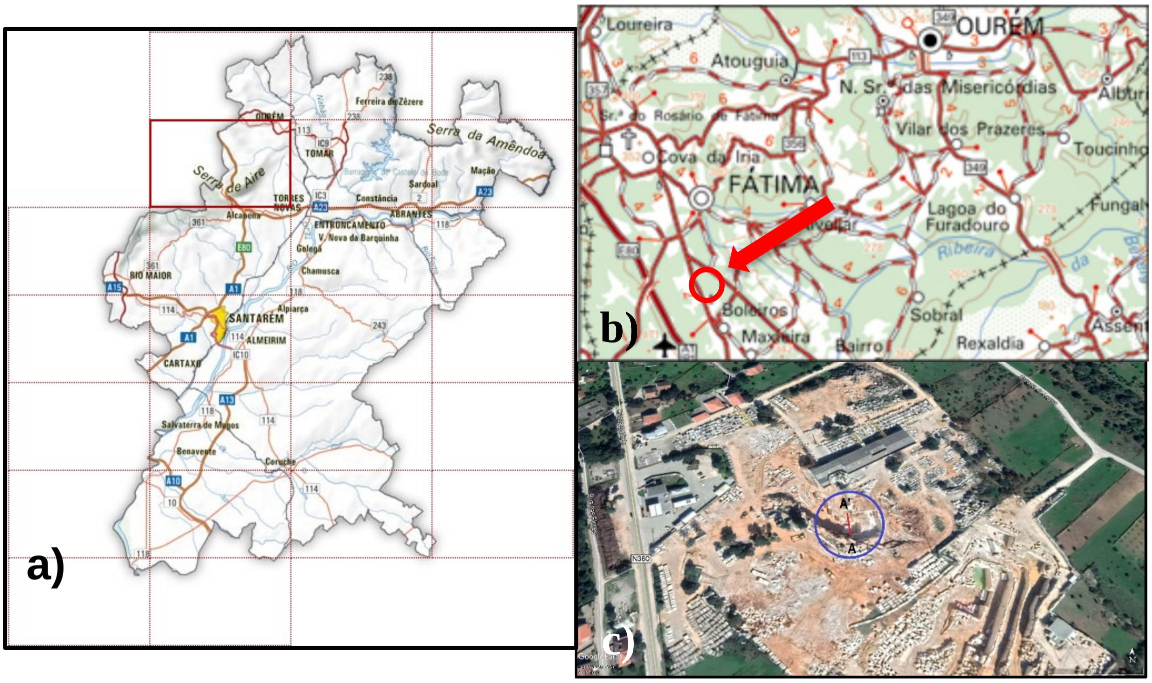

Figure 1. a) Location of the Studied area. Santarem b) Red arrow – Location in the excerpt from the map (Carta militar de Portugal 1:25 000. Continente, série M888; 309), Serviços Cartográficos do Exército; Instituto Geográfico e Cadastral) Accessed 27/06/2020. c) Blue circle – Profiles location in Valinho de Fátima (EM&R quarry), *Google Earth* image.

3. Methods and methodologies

To perform the work, several methods were used, which allowed the 3D modelling of the acquired data and its visualization integrated into the rocky massif, according to the proposed methodology and expressed in the schedule of figure 2.

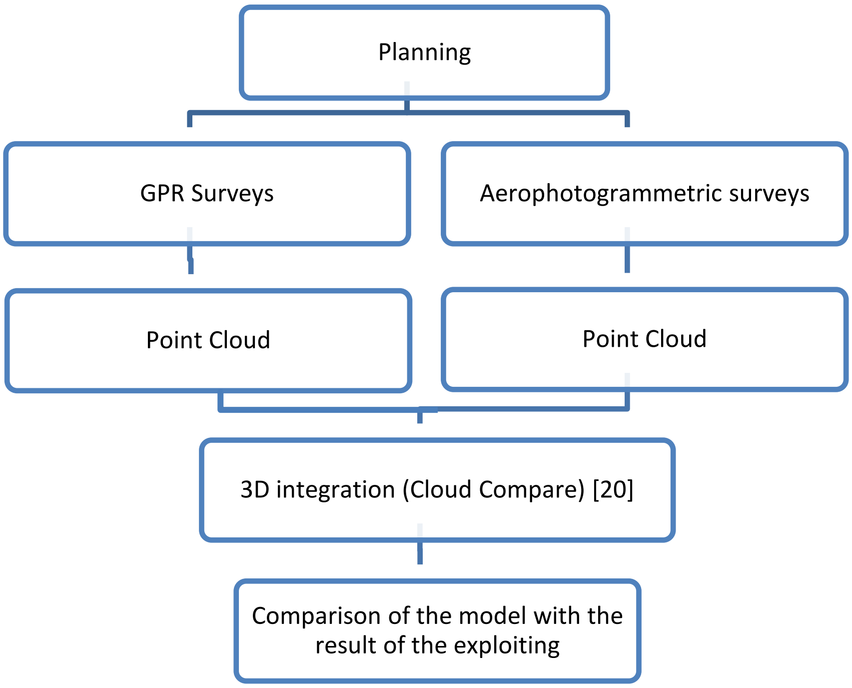

Figure 2. Methodology workflow

3.1. Ground Penetrating Radar survey

The geophysical method used was the GPR, using PULSEEKKO GPR SENSORS & SOFTWARE equipment (Figure 3 a)) with the configuration described in Table 1. For this purpose, a grid was designed on the quarry floor (Figure 3 a)) with a length of 7 meters (m), a width of 5 m and spacing between profiles of 1 m, in the place marked by the red circle and polygon (Figure 3 b)).

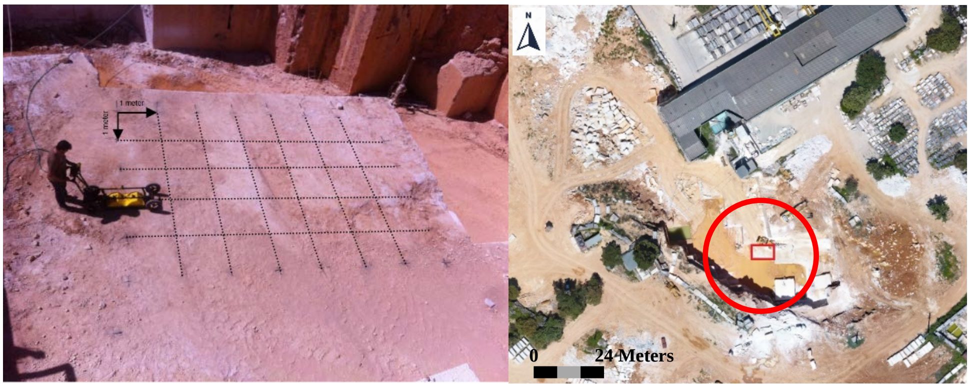

Figure 3. a) Equipment and acquisition grid on the floor of the quarry. b) Location of the area surveys in the quarry (red polygon and circle)

Table 1. Equipment Configuration Parameters

Profiles	
Data Collected	2019-Jun-05
Survey Type	Reflection
Acquisition mode and trigger	Continuous, odometer
Antenna type	Bi-static, shielded
Frequency (Mhz)	250.00
Time Window (ns)	140.00
Wave velocity (m/ns)	0.120 m/ns
Step Size (m)	0.050
Antenna Separation (m)	0.40
Dynamic Stacking (medium value)	40
Maximum depth of investigation (m)	±7.20

The GPR method is an active EM geophysical method for the acquisition and recording of in-depth information from the subsoil. It works by sending a small electromagnetic energy impulse in depth along the subsoil, with a certain frequency, from a transmitting antenna (TX), and records the intensity and time of the return of that same impulse that reaches the receiving antenna (RX) [11], [12]. After penetrating underground and along their path between the TX and RX antenna, electromagnetic impulses undergo phenomena of reflection, refraction, attenuation and absorption, these intrinsically linked to the properties of electrical conductivity, dielectric permissiveness and magnetic permeability of materials traversed by that same wave/impulse EM (Figure 4) [13].

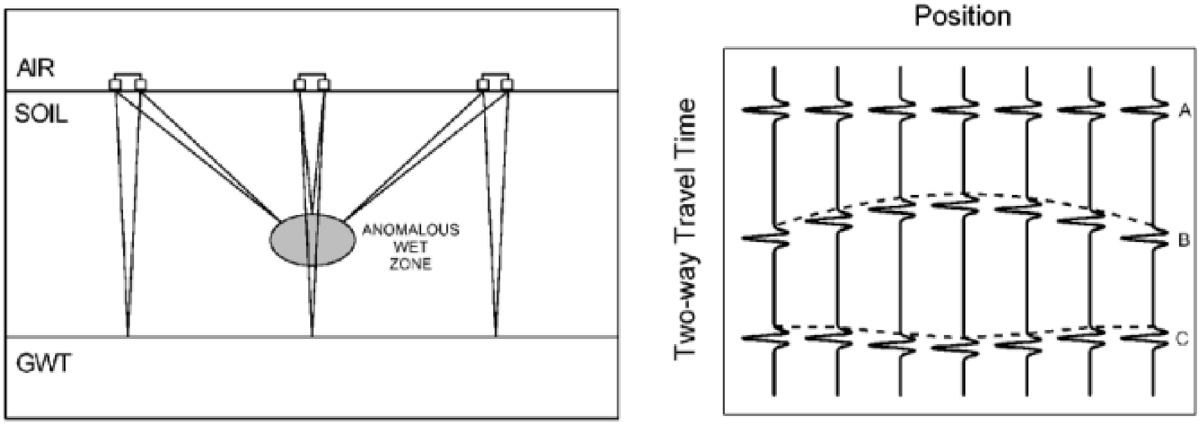

Figure 4. Idealized ground penetrating radar (GPR) transect measured with a fixed antenna separation over an anomalous wetter zone and a horizontal groundwater table (GWT). A marks the air wave, B marks the point reflector, and C marks the reflection from the groundwater table (after Davis and Annan, 1989).

Thus, the time of sending and returning a signal in depth (velocity of wave propagation in the middle) indicates to us the apparent depth to which a given target/discontinuity is found between materials, and the contrast in the amplitude/intensity and aspect of the reflection of that signal at that point indicates the differences between the dielectric properties between these material means, structures and objects (the greater the contrast between them, the greater the amount of electromagnetic energy reflected in this point).

According to the works of [12] Jol (2008) and described by [14] Lourenço *et al*. (2012) we have to, using a generator that emits electromagnetic wave impulses from a TX antenna, these waves are diffused from that same antenna to the study medium/material, where they propagate with a speed determined mainly by the electrical permissiveness of the medium (ε). When they find objects or boundaries between mediums with different electrical properties (high EM impedance result from dielectric contrast), they suffer deviations by refraction, reflection and diffraction. Part of this emitted radiation returns to the surface, where it is picked up by an RX antenna, and stored in the form of computer data in the control unit.

For GPR data processing, it was used GPR-Slice [15], where it was set an XY-GRID, data was split into 2 channels, then re-joined. Data was wobble corrected (DC removal and Dewow), time zero corrected, applied suited bandpass filter and gain, and removed background noise. For further analysis, it was applied to migration and performed Hillbert transform to envelope data. After energy balancing/normalization between survey lines, three 3D grids were then computed (filtered, migrated, and enveloped data) and geologic interpretation was done.

3.2. Aerophotogrammetric survey

The aerophotogrammetric method used for data acquisition a UAV DJI Phantom 4, which comes equipped with a camera with the specifications indicated in table 2.

Table 2. UAV Camera Specifications

Brand	Model	Nr. Pixels	Focal length (f)	Maximum aperture (F)	Sensitivity (ISO)
DJI	FC330	12.4 Mpix	f = 3.6mm (~20 mm on 35mm eq.)	F2.8 / F11	100 – 1600

Unmanned aerial vehicles (UAVs), which include the platform and control systems, are a technology with great expansion and a diversity of uses, ranging from aerial surveillance, engineering applications (mapping, monitoring of infrastructure and the environment) to a 3D mapping of geologic structures [16], [17] From the data collected, orthophoto maps, digital surface or terrain models (MDS or extracted MDT) [18] and 3D models can be produced.

As a data acquisition methodology, the flight held on 14 May 2019, was initially planned for a longitudinal overlap of 75% and a lateral overlap of 65%, in the Drone & UAV Mapping Platform application (Figure 5a)), the rest being planned according to the parameters defined in figures 5b), 5c) and flight plan set out in Figure 5d) for the proposed objectives.

The photogrammetric survey modelling was performed using the software program Alicevision Meshroom [19], which is based on the Structure from Motion (*SfM*) and dense correlation technique [20].

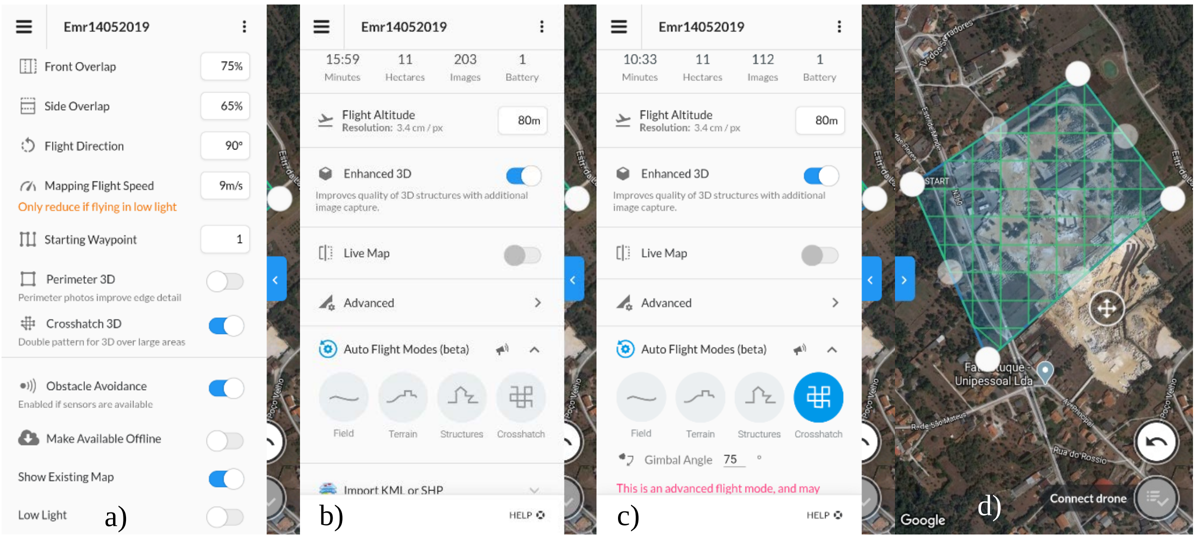

a)

Emr14052019

Front Overlap 75%

Side Overlap 65%

Flight Direction 90°

Mapping Flight Speed 9m/s

Only reduce if flying in low light

Starting Waypoint 1

Perimeter 3D ○

Perimeter photos improve edge detail

Crosshatch 3D ●

Double pattern for 3D over large areas

Obstacle Avoidance ●

Enabled if sensors are available

Make Available Offline ○

Show Existing Map ●

Low Light ○

b)

Emr14052019

15:59 Minutes 11 Hectares 203 Images 1 Battery

Flight Altitude 80m

Resolution: 3.4 cm / px

Enhanced 3D ●

Improves quality of 3D structures with additional image capture.

Live Map ○

Advanced

Auto Flight Modes (beta)

Import KML or SHP

c)

Emr14052019

10:33 Minutes 11 Hectares 112 Images 1 Battery

Flight Altitude 80m

Resolution: 3.4 cm / px

Enhanced 3D ●

Improves quality of 3D structures with additional image capture.

Live Map ○

Advanced

Auto Flight Modes (beta)

Crosshatch

Gimbal Angle 75 °

This is an advanced flight mode, and may

d)

Figure 5. a) Flight specification. Overlap. b) Flight specification. Altitude and flight mode. c) Flight specification. Angle of the chamber. d) Flight plan

4. Results and discussions

The results were very satisfactory. GPR had a high S/N ratio, and with minimum processing, inner geologic features were viewable directly/interpreted in radargrams (Figure 6).

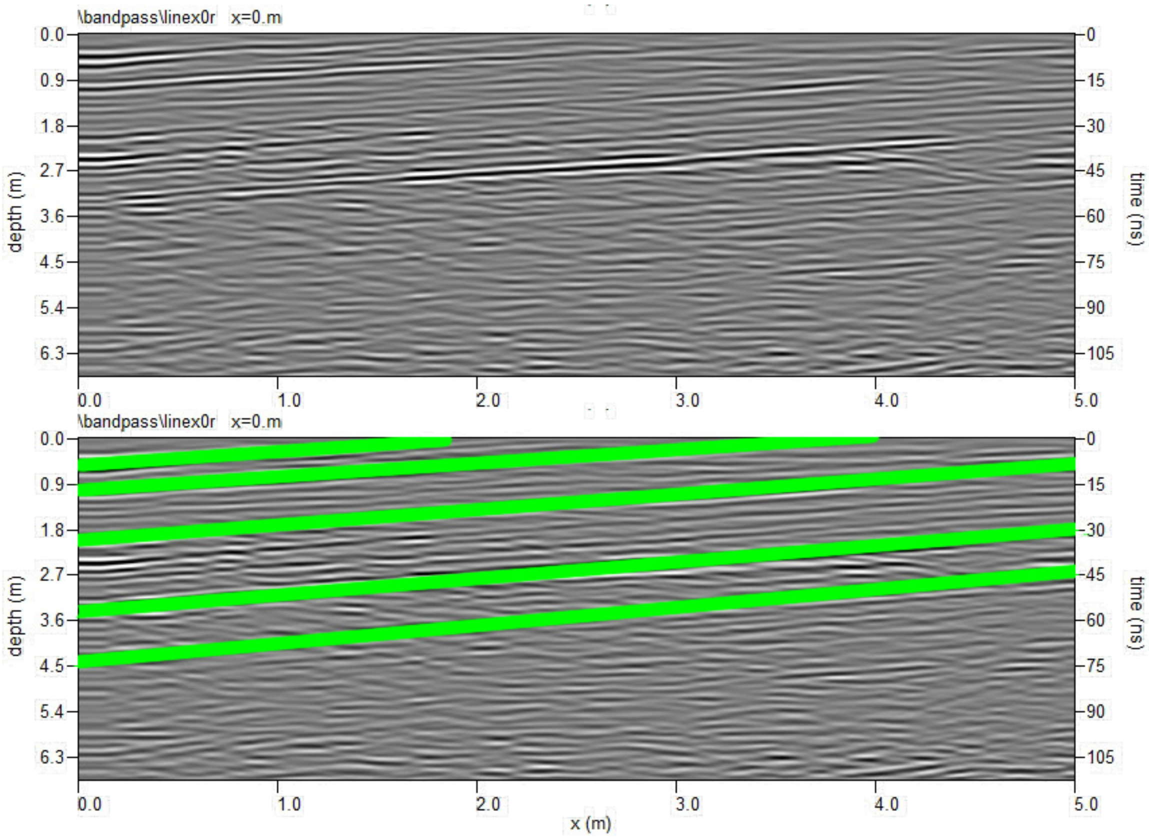

Figure 6. Filtered radargram (top) and interpreted radargram (bottom; noticeable stratification)

2D radargrams, in lines and crosslines, were processed and interpreted in their filtered, migrated, and enveloped form (Figure 7), and after interpolation between survey lines into a 3D volume dataset, further interpretation was carried (Figure 8).

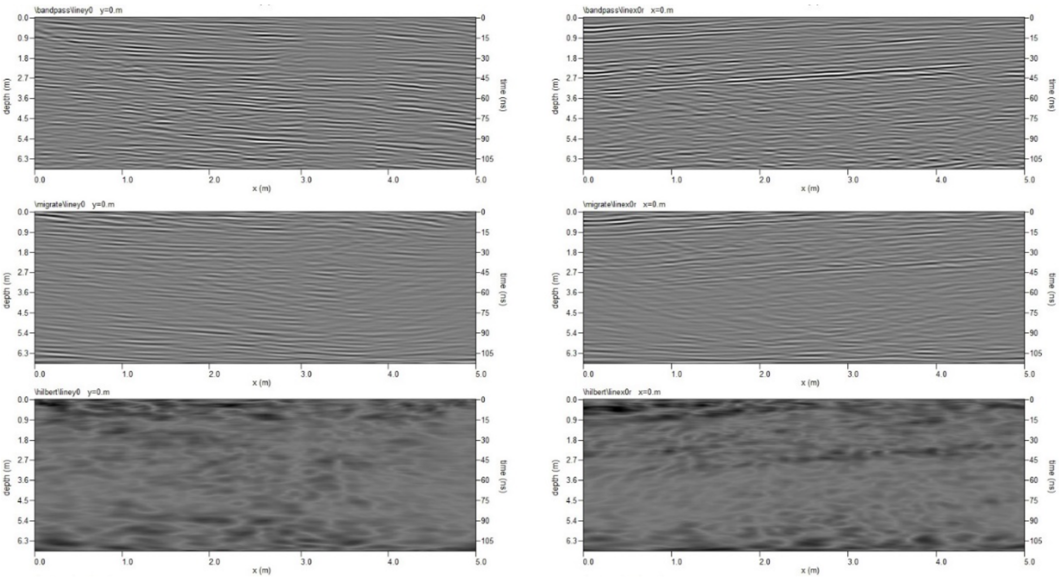

Figure 7. Sample of filtered (top), migrated (middle), enveloped (bottom) inline (left) and crossline (right)

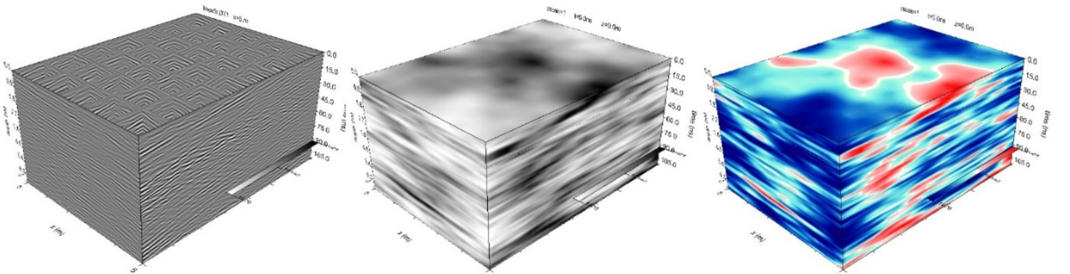

Figure 8. 2D radargrams projected in 3D (left), Enveloped volume with gray colourmap (middle), Envelope volume with colourmap (right)

Combined interpretation of 2D and 3D data was carried to assess the presence of any discontinuities (other than stratification and cross-stratification), voids, bodies, or different geology (geologic contacts), or any other disturbance, detected by the geophysical survey, that could affect negatively and cause an impact on the block value and consequent viability (Figure 9).

The GPR 3D data volume was integrated for visual inspection and 3D analysis in *CloudCompare* [21], with the photogrammetric point cloud (Figure 10) and compared to a quarry fronts (Figure 11).

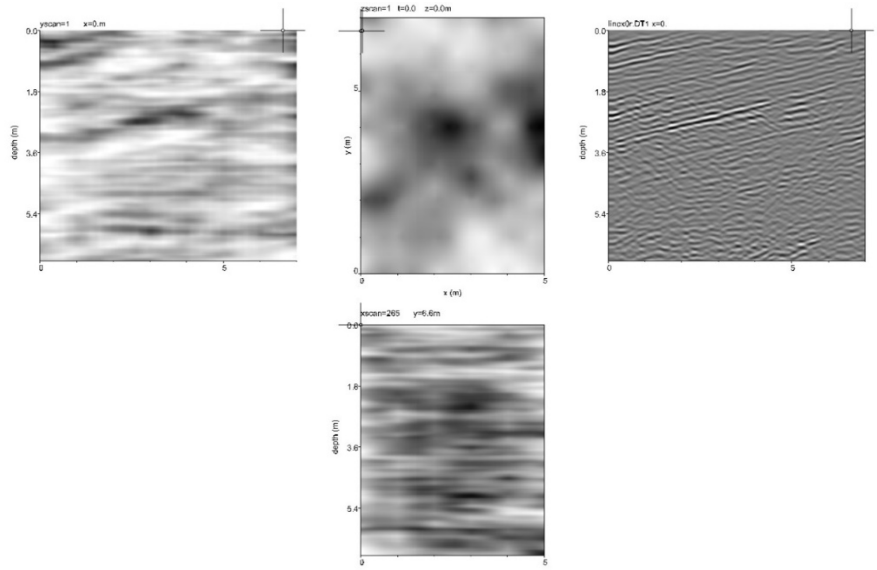

Figure 9. Combined 3D GPR visualization and interpretation

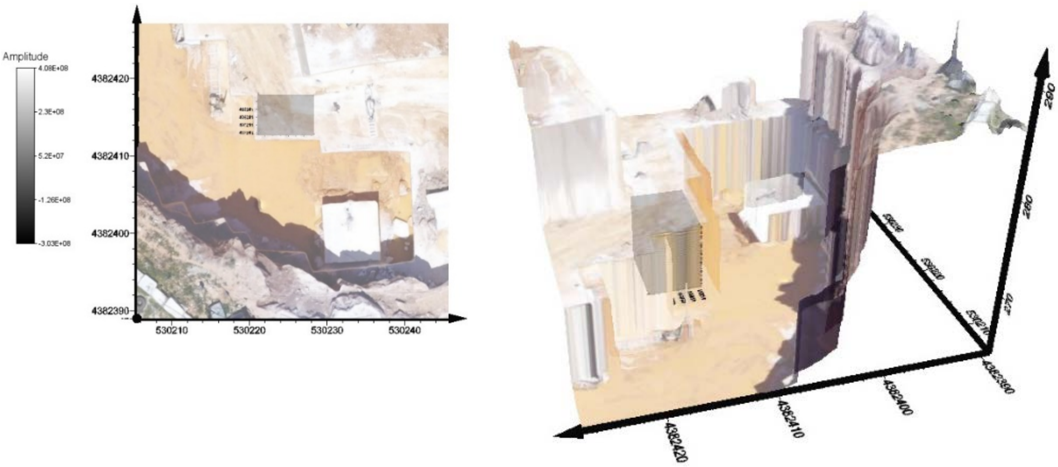

Figure 10. 3D Data integration, visualization and interpretation. Plant view (left) and a perspective view (right)

Figure 11. Quarry fronts. Perspective (left). Location of the blueish tint, red polygon (right).

5. Conclusions

The present methodology was revealed as a fast, easy and long-term cheap technology to assess the subsurface features of a limestone block and quarry exploration.

Current technologic capabilities of fast computation, both to GPR processing and photogrammetric 3D restitution, on a consumer-grade computer, and the usage of opensource software in the workflow (photogrammetry and integration) also lowers the overall costs of these procedures.

The resultant models were integrated into a non-GIS software, but as all data were georeferenced, all models and interpretations can be easily exported to any GIS or CAD software, as it is industry standard, like QGIS or similar.

The enveloped GPR data revealed the presence of some geophysical bodies, that might be related to the inner mineral sedimentary structuration of the limestone formation (mineral/grain content, porosity moisture, or others), but when the block was cut no macrostructures were visually identified.

On the lower part of the block, visually was interpreted the presence of a blueish tint, revealing the presence of microscopic mineralogy, but without further analysis (geophysical, geochemical or mineralogical) no conclusions were made, regarding its composition or nature, as dielectric impedance was not sensed in GPR (Figure 11).

As foreseen in the final interpretations, other than cross-stratification and parallel stratification, no faults, voids or fractures were present both in the limestone block and in the final cut panels.

Further similar studies will continue in the same quarry, to correctly assess and redesign (if needed) the exploration plan, avoiding, when detected, the presence of faults, fractures, or similar morphostructural discontinuities.

Acknowledgment(s)

Our thanks to IQGeo-Serviços, and the company Eduardo Marques & Rosa for the opportunity and conditions made available for the realization of this work. We also thank the financial support of FCT-MEC through national funds and, where applicable, co-financed by the FEDER under the PT2020 Partnership, through the research project UID/MULTI/00073/2013 of the Centre of Geosciences. Thanks to Geosurveys Angola, for allowing the use of GPR-Slice software for the processing of GPR data.

References

[1] J.M. Carvalho, C. Prazeres, J.V. Lisboa, and R. Sardinha, Rochas ornamentais do Maciço Calcário Estremenho: breve caraterização dos recursos, dos centros de produção e delimitação preliminar de áreas potenciais. Boletim de Minas, 47 (1), páginas 5 a 26, 2012 (in Portuguese).
[2] M. Elkarmoty, F. Tinti, S. Kasmaeeyazdi, S. Bonduà, and R. Bruno, 3D modeling of discontinuities using GPR in a commercial size ornamental limestone block. Construction and Building Materials, 166, 81-86, 2018.
[3] J. Duarte, J. Carvalho, and F. Figueiredo, Use of Ground Penetration Radar (GPR) in the Evaluation of Geological-Structural Elements of Ornamental Carbonated Rocks-Case Study in Valinho De Fatima, Portugal. In IOP Conference Series: Earth and Environmental Science (Vol. 362, No. 1, p. 012101). IOP Publishing, 2019.
[4] J. Duarte, D. Pedrosa, J. Carvalho, F. Figueiredo, and L. Catarino, Use of Non-Destructive Methods in Structural Analysis of Petrous Materials-Ultrasonic Testing and Ground Penetrating Radar (GPR). In IOP Conference Series: Earth and Environmental Science (Vol. 221, No. 1, p. 012061). IOP Publishing, 2019.

[5] R. Moura, and M.S. Matias, “Radar de Penetração (GPR: Ground Penetrating Radar) aplicado ao estudo de fracturação em mármores do anticlinal de Estremoz (Alentejo – Portugal)”, Comunicações Instituto Geológico Mineiro, tomo 86, 289-300, 1999.

[6] M. Elkarmoty, F. Tinti, S. Kasmaeeyazdi, F. Giannino, S. Bonduà, and R. Bruno, Implementation of a Fracture Modeling Strategy Based on Georadar Survey in a Large Area of Limestone Quarry Bench. Geosciences, 8(12), 481, 2018.

[7] J. Rey, J. Martínez, V. Montiel, F. Cañadas, and N. Ruiz, Characterization of the sedimentary fabrics in ornamental rocks by using GPR. Near Surface Geophysics, 15(5), 457-465, 2017.

[8] Acessed web page in 27-06-2020: Carta militar de Portugal 1:25 000. Continente, série M888 ; 309), Serviços Cartográficos do Exército; Instituto Geográfico e Cadastral) [Online] Available at: https://www.igeoe.pt/index.php?id=186&p=1&distrito=14&escala=1&concelho=217&freguesia=2137 (in Portuguese)

[9] Google: Google Earth Pro, versão 7.3.3. 7699 (64-bit) [Online] 2020. Availagle at: https://www.google.com.br/earth/download/gep/agree.html

[10] A. C. Azerêdo, Formalização da litoestratigrafia do Jurássico Inferior e Médio do Maciço Calcário Estremenho (Bacia Lusitânica). Comunicações Geológicas, 94, 29-51, 2007 (in Portuguese).

[11] A. P. Annan, Ground penetrating radar – Principles, procedures & applications. Sensors & Software Inc. Canada, 2003.

[12] H. M. Jol, Ground penetrating radar: Theory and applications. 1st edition. Elsevier Science, 2009.

[13] Huisman, J. A., Hubbard, S. S., Redman, J. D., & Annan, A. P. (2003). Measuring soil water content with ground penetrating radar: A review. Vadose zone journal, 2(4), 476-491.

[14] V. Lourenço, B. Caldeira, J. Rocha, M. Bezzenghoud, and J.F. Borges, Aplicação do Radar de Penetração no Solo (GPR) na detecção de estruturas no âmbito nas Ciências Forenses. Gazeta da Física, 34(3-4), 8-13, 2012 (in Portuguese).

[15] GPR-Slice (version 7.MT). [Online] 2020. Available at: https://www.gpr-survey.com/

[16] Y. Vasuki, E. Holden, P. Kovesi, and S. Micklethwaite, Semi-automatic mapping of geological structures using UAV-based photogrammetric data: An image analysis approach: Computers & Geosciences, v. 69, p. 22–32, 2014, DOI: 10.1016/j.cageo.2014.04.012.

[17] J. A. M. Duarte, Caracterização de áreas com potencial para extracção de rochas ornamentais carbonatadas: análise integrada de dados de fotogramétricos, geológicos e geofísica para caracterização de alta resolução de maciços rochosos carbonatados (Doctoral dissertation, Universidade de Coimbra), (in Portuguese).

[18] A.F. Habib, E.M. Kim, and C.J Kim, New methodologies for true orthophoto generation. Photogrammetric Engineering & Remote Sensing, 73(1), 25-36, 2007.

[19] L. Kneip, D. Scaramuzza, and R. Siegwart, A novel parametrization of the perspective-three-point problem for a direct computation of absolute camera position and orientation. In CVPR, IEEE Computer Society Conference on Computer Vision and Pattern Recognition. IEEE Computer Society Conference on Computer Vision and Pattern Recognition, 2969–2976. 06 2011. DOI:10.1109/CVPR.2011.5995464

[20] M.J. Westoby, J. Brasington, N.F. Glasser, M.J. Hambrey, and J.M. Reynolds, ‘Structure-from-Motion’photogrammetry: A low-cost, effective tool for geoscience applications. Geomorphology, 179, 300-314, 2012.

[21] CloudCompare (version 2.11.0) [GPL software], [Online] 2020. Available at: http://www.cloudcompare.org/